Carbohydrate Polymers 91 (2013) 508–517

Contents lists available at SciVerse ScienceDirect

Carbohydrate Polymers

journal homepage: www.elsevier.com/locate/carbpol

Effects of molecular weight and pyridinium moiety on water-soluble chitosan derivatives for mediated gene delivery

Warayuth Sajomsang[a,*], Pattarapond Gonil[a], Uracha Rungsardthong Ruktanonchai[a], Maleenart Petchsangsai[a], Praneet Opanasopit[b], Satit Puttipipatkhachorn[c]

[a] National Nanotechnology Center, National Science and Technology Development Agency, Pathumthani, Thailand
[b] Pharmaceutical Development of Green Innovations Group (PDGIG), Faculty of Pharmacy, Silpakorn University, Nakhon Pathom, Thailand
[c] Department of Manufacturing Pharmacy, Faculty of Pharmacy, Mahidol University, Bangkok, Thailand

ARTICLE INFO

Article history:
Received 14 May 2012
Received in revised form 16 August 2012
Accepted 16 August 2012
Available online 24 August 2012

Keywords:
Chitosan
Quaternized chitosan
Methylated *N*-(3-pyridylmethyl) chitosan chloride
Molecular weight
Pyridinium/trimethyl ammonium ratio
Gene delivery

ABSTRACT

The aim of this study is to investigate the effects of molecular weight, the pyridinium/trimethyl ammonium (Py/Tr) ratio, the nitrogen atoms (N) in the methylated *N*-(3-pyridylmethyl) chitosan chloride (M3-PyMeChC)/the phosphorus atoms (P) in DNA (N/P) ratio, and the physicochemical properties of nanopolyplexes on transfection efficiency. The water-soluble chitosan derivative, M3-PyMeChC, was used as a non-viral vector to deliver pEGFP-C2 into human hepatoma (Huh7) cell lines. The results revealed that higher molecular weight M3-PyMeChC was able to form complexes completely with DNA at lower N/P ratios than that with lower molecular weights, which led to higher transfection efficiency. Moreover, the M3-PyMeChC with higher Py/Tr ratios showed superior transfection efficiency at lower Py/Tr ratios at all N/P ratios studied. The highest transfection efficiency for the nanopolyplexes occurred for a molecular weight of 82 kDa at a N/P ratio of 5. The results indicated that the hydrophobic effect of pyridinium moiety could enhance gene transfection efficiency, which can be attributed to the dissociation of DNA from nanopolyplexes. High Py/Tr ratios in nanopolyplexes tended to decrease cytotoxicity due to delocalization of positive charge into a pyridine ring while high N/P ratios and molecular weight increased cytotoxicity. Our results showed that the vector was able to spread the positive charge by delocalizing it into a heterocyclic ring, suggesting to a promising approach to mediate higher levels of gene transfection.

1. Introduction

Gene therapy is the insertion of genes into a specific cell and tissue to treat or prevent disease. It may be used to replace a faulty gene or to introduce a new gene whose function is to cure a disease. An ideal gene delivery method needs to meet 3 major criteria: (1) it should protect the transgene against degradation by nucleases in intercellular matrices, (2) it should bring the transgene across the plasma membrane and into the nucleus of target cells, and (3) it should have no detrimental effects (Gao, Kim, & Liu, 2007). There are two approaches for gene delivery: viral and non-viral. Viral delivery is a conventional approach because viruses have evolved to infect cells with high efficacy. However, clinical trials have underscored the safety risks of viral gene delivery due to the possibility of causing cancer and death (Green, Langer, & Anderson, 2008). For this reasons, much attention has been focused on the non-viral approach due to its potentials to overcome many inherent challenges of viral vectors. Numerous non-viral gene vectors which have several advantages over their viral counterparts, including ease of production, low immune response, the ability to transfer large DNA molecules and potential cell targeting properties, have been developed for gene delivery (Anderson, 1992; Li & Huang, 2000). However, a disadvantage of non-viral gene vectors is their low transfection efficiencies compared to viral vectors. In order to improve the transfection efficiency, numerous cationic polymers such as polyethyleneimine (PEI), poly(L-lysines) (PLL), poly(2-(dimethylamino)ethylmethacrylate) (PDMAEMA), and chitosan (Ch) have been studied for *in vitro* as well as *in vivo* applications (Kim et al., 2007). Despite PEI having excellent transfection efficiency, it is not an ideal carrier because it is not biodegradable and it can cause considerable cytotoxicity via necrosis and apoptosis (Boussif et al., 1995). Chitosan is one of the candidates for use as a non-viral vector due to its non-toxic, biocompatible, and biodegradable properties in the human body. Moreover, it has been proposed as a safer alternative to

* Corresponding author at: National Nanotechnology Center, Nanodelivery System Laboratory, National Science and Technology Development Agency, Thailand Science Park, Pathumthani 12120, Thailand. Tel.: +66 2 564 7100; fax: +66 2 564 6981.
E-mail address: warayuth@nanotec.or.th (W. Sajomsang).

0144-8617/$ – see front matter © 2012 Elsevier Ltd. All rights reserved.
http://dx.doi.org/10.1016/j.carbpol.2012.08.053

other non-viral carrier such as cationic lipids and other cationic polymers (Jayakumar et al., 2010; Weecharangsan, Opanasopit, Ngawhirunpat, Rojanarata, & Apirakaramwong, 2006). However, the applications of chitosan are still limited due to its insolubility in water. In addition, the low specificity and transfection efficiency of chitosan has to be overcome before it can be used in clinical trials (Kim et al., 2007).

Since pyridinium amphiphiles have been shown to be non-toxic for *in vitro* gene delivery (Ilies et al., 2004; Pijper et al., 2003; Van Der Woude et al., 1997), the need to improve the water solubility and gene transfection efficiency of chitosan has led to the development of the pyridinium chitosan derivatives (Opanasopit et al., 2008; Sajomsang, Ruktanonchai, Gonil, Mayen, & Opanasopit, 2009). In this study, methylated *N*-(3-pyridylmethyl) chitosan chloride (M3-PyMeChC) was used as a model gene vector and the effects of molecular weight ranging from 82 to 18 kDa, pyridinium/trimethyl ammonium (Py/Tr) ratios of 16 ± 2 and 0.8 ± 2, and their physicochemical properties on gene transfection efficiency were investigated.

2. Materials and methods

2.1. Materials

The chitosan (Ch), which was purchased from Seafresh Chitosan Lab (Bangkok, Thailand), had a molecular weight of 276 and 16 kDa and degree of deacetylation (DDA) of $94 \pm 2\%$. Sodium cyanoborohydride and polyethylenimine (PEI), with a molecular weight of 25 kDa, were purchased from Aldrich (Milwaukee, USA). Iodomethane, 3-pyridinecarboxaldehyde, sodium iodide, and 1-methyl-2-pyrrolidone (NMP) were sourced from Fluka (Deisenhofen, Germany). Sodium nitrite and hydrochloric acid were purchased from Carlo Erba Reagent (Italy). 3-(4,5-Dimethylthiazol-2-yl)-2,5-diphenyl tetrazolium bromide (MTT) was purchased from Sigma-Chemical Co. (St. Louis, MO, USA). Dulbecco's modified Eagle's medium (DMEM), Trypsin–EDTA, penicillin–streptomycin antibiotics, and fetal bovine serum (FBS) were obtained from GIBCO-Invitrogen (Grand Island, NY, USA). The human hepatocellular carcinoma (Huh7) cell lines were obtained from the American Type Culture Collection (ATCC, Rockville, MD, USA). All other chemicals were of cell culture and molecular biology grade.

2.2. Synthesis of 3-PyMeCh

N-(3-pyridylmethyl) chitosan (3-PyMeCh) with different molecular weights and degrees of N-substitution (DS) were prepared by reductive amination according to the previously reported procedure (Sajomsang, Rungsardthong Ruktanonchai, Gonil, & Warin, 2010). Briefly, chitosan was dissolved in 1% (v/v) of acetic acid, and then ethanol was added. After that, 3-pyridinecarboxaldehyde at different mole ratios was added and stirred at room temperature for 24 h. The pH of the solution was adjusted to 5 with 15% (w/v) of NaOH. Subsequently, $NaCNBH_3$ was added and stirred at room temperature for 24 h, followed by pH adjustment to 7 with 15% (w/v) of NaOH. The reaction mixture was then dialyzed in deionized water (DI) for 3 days in order to remove any impurity and freeze-dried to produce powdered 3-PyMeCh. The DS was determined by ^{1}H NMR spectroscopy.

2.3. Methylation of 3-PyMeCh

A mixture of 3-PyMeCh and NMP was stirred at room temperature for 12 h. Then 15% (w/v) of sodium hydroxide and sodium iodide were added and stirred at 60 °C for 15 min. Subsequently, iodomethane was added in three portions at 3 h intervals and stirred at 60 °C for 24 h. The reaction mixture was precipitated in acetone. The precipitate was then dissolved in 15% (w/v) of NaCl in order to replace the iodide ions with chloride ions. After that the suspension was dialyzed with DI water for 3 days to remove inorganic materials and then freeze-dried to obtain a yellow cotton-like 3-PyMeChC power. The chemical structures of M3-PyMeChC with different pyridinium/trimethyl ammonium (Py/Tr) ratios are shown in Fig. 1.

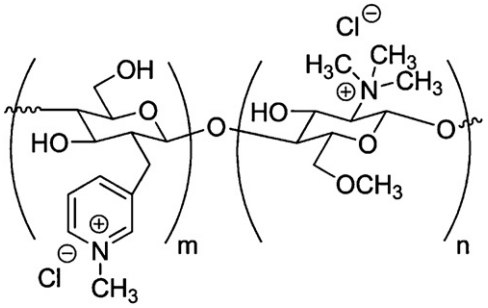

Fig. 1. Chemical structure of M3-PyMeChC with Py/Tr = 16 ± 2 when $m \gg n$ and Py/Tr = 0.8 ± 2 when $m < n$.

2.4. Analytical methods

2.4.1. ATR-FTIR and ^{1}H NMR spectroscopy

All attenuated total reflectance Fourier transform infrared (ATR-FTIR) spectra were collected with a Nicolet 6700 spectrometer (Thermo Company, USA) using the single-bounce ATR-FTIR spectroscopy (Smart Orbit accessory) with a diamond internal reflection element (IRE) at the ambient temperature (25 °C). These spectra were collected using rapid-scan software in an OMNIC 7.0 utilizing 32 scans and a resolution of 4 cm^{-1}. The ^{1}H NMR spectra were measured on a Bruker AVANCE 500 MHz spectrometer (Bruker, Switzerland). All measurements were performed at 300 K, using pulse accumulation of 64 scans and a LB parameter of 0.30 Hz. 1% (v/v) D_2O/CF_3COOD and D_2O were utilized as solvents for 5–10 mg chitosan and its methylated derivatives, respectively.

2.4.2. Determination of molecular weight

The weight average molecular weight (M_w), number average molecular weight (M_n), and M_w/M_n of chitosan and its methylated derivatives were determined using the gel permeation chromatography (GPC). The equipment consisted of a Waters 600E Series generic pump, an injector, ultrahydrogel linear columns (M_w resolving range 1–20,000 kDa), a guard column, standard pollulans (M_w of 5.9–788 kDa), and a refractive index detector (RI). All samples were dissolved in acetate buffer with a pH of 4 and then filtered through VertiPure 0.45 μm nylon syringes filters (Vertical Chromatography Co., Ltd., Thailand). The mobile phases, 0.5 M AcOH and 0.5 M AcONa (acetate buffer pH 4), were used at a flow rate of 0.6 mL/min at 30 °C. Then an injection volume of 20 μL was used.

2.4.3. Determination of size and zeta potential

The *Z*-average hydrodynamic diameter, polydispersity index (PDI) and surface charge of the nanopolyplexes were determined by dynamic light scattering (DLS) using a Zetasizer Nano ZS (Malvern Instruments Ltd., Malvern, UK). The mixtures (1 mL) containing 1 μg of pEGFP-C2 were prepared at N/P ratios ranging from an amount that exhibited incompletely binding to an excess of M3-PyMeChC. The refractive index of chitosan and the viscosity of DI water for were used in the calculations. All samples were measured at 25 °C in triplicate.

2.4.4. Transmission electron microscopy (TEM)

The morphologies of nanopolyplexes at optimal N/P ratios were observed by a transmission electron microscopy (TEM, JEM-100CX II, Japan). The nanopolyplexes were diluted to a total volume of 100 μL with a 0.15 M NaCl solution and then incubated at 37 °C for 30 min. A TEM sample was prepared by dipping a copper grid with a Formvar film into the freshly prepared nanoparticle solution. After the deposition, the aqueous solution was blotted away with a strip of filter paper and dried in air.

2.5. Acid–base titration

The buffer capacity of M3-PyMeChC was determined by acid–base titration assay (Benns, Choi, Mahato, Park, & Kim, 2000). Briefly, 20 mg of each sample was dissolved in 50 mL of 150 mM NaCl solution. The sample solution was firstly titrated with 0.1 M NaOH to a pH of 10, and then 0.1 M HCl solution was added to the solution to obtained mixtures with different pH values which were determined using a METLER TOLEDO T50 Titration Excellence with a DG115-SC sensor.

2.6. Preparation of plasmid DNA and bacterial culture

The plasmid DNA used was pEGFP-C2 (Clontech, Palo Alto, USA), encoding green fluorescent protein (GFP) which was originally cloned from the mutant *Aequorea victoria*. The pEGFP-C2 was amplified in a *Escherichia coli* DH101 strain which was cultured in Luria–Bertani (LB) broth 1% (w/v) tryptone, 0.5% (w/v) yeast extract (Difco, USA), 0.5% (w/v) NaCl (Molekula, UK) containing 0.015 mg/mL kanamycin (GIBCO, USA) and then grown at 37 °C with shaking at 250 rpm. The pEGFP-C2 was extracted from bacterial culture using QIAGEN Hispeed plasmid midi kits (Qiagen, Germany). The purity, concentration and size of plasmid DNA were examined through comparison with the MassRuler DNA ladder mix (Fermentas, USA) for optical densities of 260 and 280 nm and by 1% agarose gel electrophoresis in Tris–boric acid–EDTA (TBE) buffer (BioRad, USA).

2.7. Preparation of nanopolyplexes

The preparation of nanopolyplexes was calculated from the N/P ratios of moles of nitrogen atom in M3-PyMeChC relative to those of the phosphate atoms in DNA. The N/P ratios were calculated according to Eq. (1).

$$\mathrm{N/P} = \frac{[\text{Mass of M3-PyMeChC} \times \text{Average repeat unit molecular weight of DNA}]}{[\text{Mass of DNA} \times \text{Average repeat unit molecular weight of M3-PyMeChC}]} \times 100 \quad (1)$$

where N/P is the ratio of nitrogen atoms in the M3-PyMeChC to phosphorus atoms in the DNA. Eq. (1) assumes that there is only one ionizable nitrogen group per repeat unit of the polymer. The M3-PyMeChC was dissolved in distilled water, followed by an addition of pDNA and incubated for 15 min at room temperature. The N/P ratios of the nanopolyplexes varied from 0.3 to 20.

2.8. Gel retardation assay

To determine the capacity of M3-PyMeChC to bind with pEGFP-C2, the amount of M3-PyMeChC was varied to investigate the appropriate N/P ratio for nanopolyplexes within the range 0.3–20. The mixture (10 μL) containing deionized (DI) water, pEGFP-C2, and M3-PyMeChC were mixed by pipetting and vortexing then the complexes were allowed to form at room temperature for 15 min. The nanopolyplexes (10 μL) containing 1 μg of pDNA were loaded in each well of 1% agarose gel electrophoresis with a Tris–boric acid–EDTA (TBE) buffer running 100 V for 40 min. The samples were analyzed under a UV transilluminator (Syngene, UK) after being stained with 1 μg/mL of ethidium bromide.

2.9. In vitro transfection studies

In vitro transfection studies were performed in Huh7 cells using pEGFP-C2 as a marker gene. Huh7 cells were seeded for 24 h into 24-well plates at a density of 5×10^4 cells/cm^2 in 1 mL of growth medium (DMEM containing 10% FBS, supplemented with 2 mM L-glutamine, 1% non-essential amino acid solution, 100 U/mL penicillin and 100 μg/ml streptomycin). The cells were grown under a humidified atmosphere (5%CO_2, 95% air and 37 °C) for 24 h. Prior to transfection, the medium was removed and the cells were rinsed with phosphate-buffered saline (PBS, pH 7.4). The cells were incubated with 0.5 mL of the nanopolyplexes containing 1 μg of pDNA for 24 h at 37 °C under a 5%CO_2 atmosphere at various N/P ratios. Non-treated cells, cells transfected with naked plasmid and PEI/DNA nanocomplexes with a N/P ratio of 8 were used as controls. After transfection, the cells were washed with PBS twice and grown in a culture medium for 48 h to allow GFP expression. The fluorescent intensity was determined using a flow cytometer (BD Facscalibur™, Germany). All transfection experiments were performed in triplicate.

2.10. In vitro cell viability assay

The evaluation of *in vitro* cytotoxicity was performed by MTT assay. Huh7 cells were seeded in a 96-well plate at a density of 5×10^4 cells/cm^2 in 200 μL of growth medium and incubated for 24 h at 37 °C under a 5%CO_2 atmosphere. Prior to transfection, the medium was removed and the cells were rinsed with PBS, and then supplied with the nanopolyplexes at the same concentrations as in the *in vitro* transfection experiment. After treatment, the nanopolyplex solutions were removed. Finally, the cells were incubated with a 100 μL MTT-containing medium (1 mg/mL) for 4 h. Then the medium was removed, the cells were rinsed with PBS at a pH 7.4, and the formazan crystals formed in living cells were dissolved in 100 μL DMSO per well. Relative viability (%) was calculated based on absorbance at 550 nm using a microplate reader (Universal Microplate Analyzer, Model AOPUS01 and AI53601, Packard BioScience, CT, USA). The viability of non-treated control cells was arbitrarily defined as 100%.

2.11. Cellular uptake studies

Plasmid DNA, pEGFP-C2, was labeled with rhodamine isothiocyanate (RITC) using a Mirus labeling kit (Mirus Bio Corporation, USA). The RITC labeled-DNA was then formed into a nanopolyplex with fluorescein isothiocyanate (FITC) labeled-M3-PyMeChC with a M_w of 82 kDa. For confocal laser scanning microscopy (CLSM), Huh7 cells (10×10^4 cells/well) were seeded on cover slides which were placed on 6-well plates prior to transfection experiments. After 24 h, the cells were treated with RITC and labeled-pDNA/FITC labeled-M3-PyMeChC nanopolyplexes at a N/P ratio of 5 and incubated for 24 h. After incubation, the remaining nanopolyplexes were removed from the cells and the cells were washed twice with 2 mL of PBS. The washing process was repeated for 3 times. Then, the cells were fixed with 4% *p*-formaldehyde in PBS for 10 min at room temperature and were then washed three times with 2 mL of PBS. The nucleus of each treated cell was stained with TO-PRO-3 for 30 min at room temperature. After that, the cells were mounted with anti-fade reagent (ProLong® Gold, Invitrogen). The cells were

Table 1
Methylation and molecular weight determination of *N*-(3-pyridylmethyl) chitosan derivatives ($n = 3$).

Samples	DS (%)	DQ_T (%)		Py/Tr ratio	M_n (kDa)	M_w (kDa)	M_w/M_n	Recovery (%)
		DQ_{py} (%)	DQ_{Ch} (%)					
M3-PyMeChC	80 ± 2	80 ± 2	5 ± 2	16 ± 2	17.49	82.18	4.69	100 ± 2
M3-PyMeChC	80 ± 2	80 ± 2	5 ± 2	16 ± 2	15.80	56.62	3.58	63 ± 2
M3-PyMeChC[a]	80 ± 2	80 ± 2	5 ± 2	16 ± 2	3.50	8.44	2.41	72 ± 2
M3-PyMeChC	38 ± 2	38 ± 2	45 ± 2	0.8 ± 2	20.76	102.01	4.91	90 ± 1

Abbreviations: DS, the degree of N-substitution; DQ_{py}, the degree of quaternization at aromatic substituents; DQ_{Ch}, the degree of quaternization; DQ_T, the total degree of quaternization ($DQ_{py} + DQ_{Ch}$); Py/Tr ratio, pyridinium/trimethyl ammonium ratio.

[a] Started from chitosan with M_w = 16 kDa; recovery (%) = weight of product (g)/weight of starting reactant (g) × 100.

visualized on a FluoView 1000 Confocal Laser Scanning Microscope (CLSM) (Olympus, USA).

2.12. Statistical analysis

The statistical significance of differences in transfection efficiency and cell viability was examined using one-way analysis of variance (ANOVA) followed by an LSD post hoc test. The significance level was set at $p < 0.05$.

3. Results and discussion

3.1. Synthesis and characterization of M3-PyMeChC

The quaternary ammonium salt of the chitosan derivatives was prepared into two steps: preparation of chitosan derivatives and quaternization (methylation) of chitosan derivatives. These two steps are interchangeable. The 3-PyMeCh was synthesized by reductive amination (Sajomsang et al., 2010). The reaction took place via the Schiff base intermediate. Then the Schiff base was reduced with sodium cyanoborohydride. The degree of N-substitution (DS) was found to range from 38 ± 2% to 80 ± 2% (Table 1). Subsequently, the 3-PyMeCh was quaternized with iodomethane in the presence of NMP, sodium hydroxide and sodium iodide yielded M3-PyMeChC (Fig. 1). The total degree of quaternization (DQ_T) was found to be 85 ± 2% which was divided into two pyridinium/trimethyl ammonium (Py/Tr) ratios; Py/Tr = 16 ± 2 and Py/Tr = 0.8 ± 2 (Table 1). The chemical structures of chitosan and its derivatives were characterized by ATR-FTIR and ^{1}H NMR spectroscopy as previously reported (Sajomsang et al., 2010). The ATR-FTIR spectrum of the 3-PyMeCh was similar to that of chitosan except for the additional absorption bands at wavenumbers 1595, 1578, 1427, 788 and 707 cm^{-1}. These bands were assigned to the C=C stretching and C—H deformation (out of plane) of the aromatic group, respectively. The M3-PyMeChC exhibited the characteristic ATR-FTIR spectra at wavenumber 1472 cm^{-1}, whereas trimethyl ammonium chloride exhibited the ATR-FTIR spectra at wavenumber 1470 cm^{-1} due to the C—H symmetric bending of the methyl substituent of quaternary ammonium groups. The ^{1}H NMR spectrum of the 3-PyMeCh exhibited the multiplet proton signals at δ 8.52–7.65 ppm due to the aromatic protons, while the singlet proton signal at δ 4.59 ppm was assigned to the methylene proton adjacent to the N atom of chitosan. The ^{1}H NMR spectrum of the M3-PyMeChC exhibited a proton signal at 5.40 ppm due to the H1′ proton of the GlcN from M3-PyMeChC. The proton signals at δ 4.23, 3.20, 2.60 and 2.30 were assigned to the *N*-methyl protons of pyridinium moiety, *N*,*N*,*N*-trimethyl protons *N*,*N*-dimethyl protons, and *N*-methyl protons of GlcN, respectively. The reduction of M3-PyMeChC molecular weight was carried out using 0.1% (w/v) of sodium nitrite in aqueous hydrochloric acid and stirring for 24 h (Table 1) (Janes & Alonso, 2003; Knight, Shapka, & Amsden, 2007). The result revealed that the molecular weight of the M3-PyMeChC had been reduced from 82 kDa to 56 kDa.

3.2. Physicochemical characterization of nanopolyplexes

The binding capability of the cationic non-viral vector to DNA is a prerequisite in gene delivery system. A cationic non-viral vector is able to condense with DNA to form compact structures and to reduce the electrostatic repulsion between the DNA and the cell surface by neutralizing the negative charge, which then facilitates the uptake of the nanopolyplex to negatively charged cell membrane constituents, leading to a higher rate of cellular uptake. When DNA is condensed by a cationic non-viral vector, it also can also be better protected against enzymatic degradation by nucleases in serum and extracellular fluids (Farber & Domb, 2007). To investigate the binding capability of the M3-PyMeChC with DNA and to determine the optimal complexation conditions adequately, the solutions of M3-PyMeChC and DNA were electrophoresed on an agarose gel containing ethidium bromide (Fig. 2). All the M3-PyMeChC with a M_w of 102, 82 and 56 kDa formed nanopolyplexes with DNA at a N/P ratio of 0.3, whereas the M3-PyMeChC with a M_w of 8 kDa required a higher N/P ratio to completely bind with DNA (Fig. 2C). The results revealed that DNA binding capability was dependent on the M_w of the M3-PyMeChC used. At similar DQ values, a higher M_w for the M3-PyMeChC was superior to a lower M_w in enhancing DNA binding. This can be observed by comparing the gels retardation from the left to right in each column of Fig. 2A–D. Higher M_w for M3-PyMeChC bound DNA at a N/P ratio of 0.3, whereas a lower M_w for M3-PyMeChC required a N/P ratio of 5 to completely bind with DNA. The influence of M_w on DNA binding could be attributed to the chain entanglement effect. Longer polymer chains in the higher M_w M3-PyMeChC more easily entangled free DNA once the initial electrostatic interaction had occurred (Kiang, Wen, Lim, & Leong, 2004).

The charge and particle size of the nanopolyplexes are very important for a cationic non-viral vector, playing an important role in endosomal uptake, the cytoplasmatic transport, and the migration through the nucleopore complexes, which mediate the bidirectional transport between the cytoplasm and the nucleus (Farber & Domb, 2007). In the present study, particle sizes and zeta potentials of nanopolyplexes at various N/P ratios ranging from 0.3 to 20 were measured by mixing the M3-PyMeChC solutions with the DNA. The particle sizes and zeta potentials of nanopolyplexes at N/P ratios ranging from 0.3 to 20 are shown in Figs. 3 and 4. For complete nanopolyplex formation, the particle sizes ranged from 150 to 250 nm and tended to increase at higher N/P ratios. This is attributed to aggregation of nanopolyplexes when high concentrations of polymer are used. This is the reason why larger particle sizes for nanopolyplexes at lower M_w (8 kDa) can be observed. Initially, the negative zeta potentials were observed, which was due to incomplete condensation between M3-PyMeChC and DNA. The zeta potentials of the nanopolyplexes increased with an increase in N/P ratios. At high N/P ratios, the

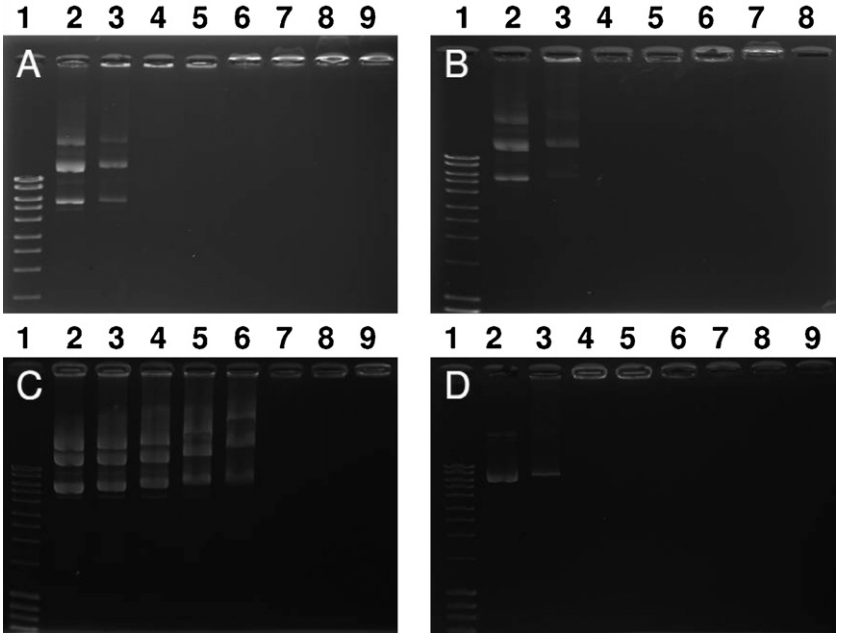

Fig. 2. Gel retardation of nanopolyplexes with $DQ_T = 85 \pm 2\%$ and $Py/Tr = 16 \pm 2$: (A) $M_w = 82$ kDa, (B) $M_w = 56$ kDa and (C) 8 kDa, and with $DQ_T = 83 \pm 2\%$ and $Py/Tr = 0.8 \pm 2$; (D) $M_w = 102$ kDa. Lane 1, DNA marker and lane 2 DNA; lanes 3–9, nanopolyplexes at N/P ratios of 0.3, 0.5, 1, 3, 5, 10, and 20, respectively.

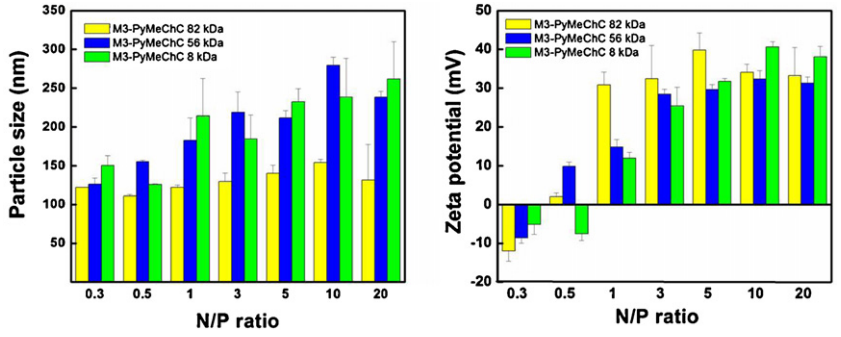

Fig. 3. The particle sizes and zeta potentials of nanopolyplexes at $DQ_T = 85 \pm 2\%$ and $P/T = 16 \pm 2$ with different molecular weights.

zeta potential was observed to reach a maximum plateau. This is due to the highly negative charge of the DNA, which was rapidly neutralized, and then the surface charge of the nanopolyplexes changed to positive values at higher N/P ratios. Moreover, there is no significant effect of molecular weight ranging from 8 to 102 kDa on zeta potential (Figs. 3 and 4). This is consistent with the results of Huang, Khor, and Lim (2004) and Kean, Roth, and Thanou (2005).

To confirm the formation of nanopolyplexes, the representative morphologies of nanopolyplexes at a N/P ratio of 5 for M_w of 56, 82 and 102 kDa, and a N/P ratio of 10 for a M_w of 8 kDa, were observed by transmission electron microscopy (TEM) (Fig. 5). All nanopolyplexes displayed a rather spherical shape. However, some nanopolyplexes were able to aggregate at high N/P ratios which were consistent with the particle sizes measured using a dynamic light scattering technique (Figs. 3 and 4). In order to investigate the

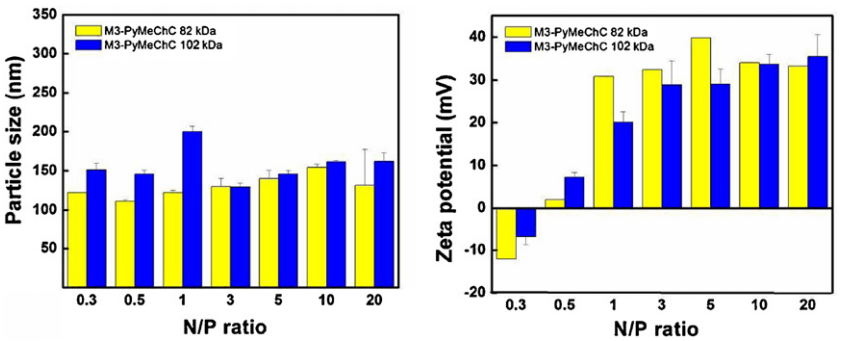

Fig. 4. The particle sizes and zeta potentials of nanopolyplexes with different Py/Tr ratios.

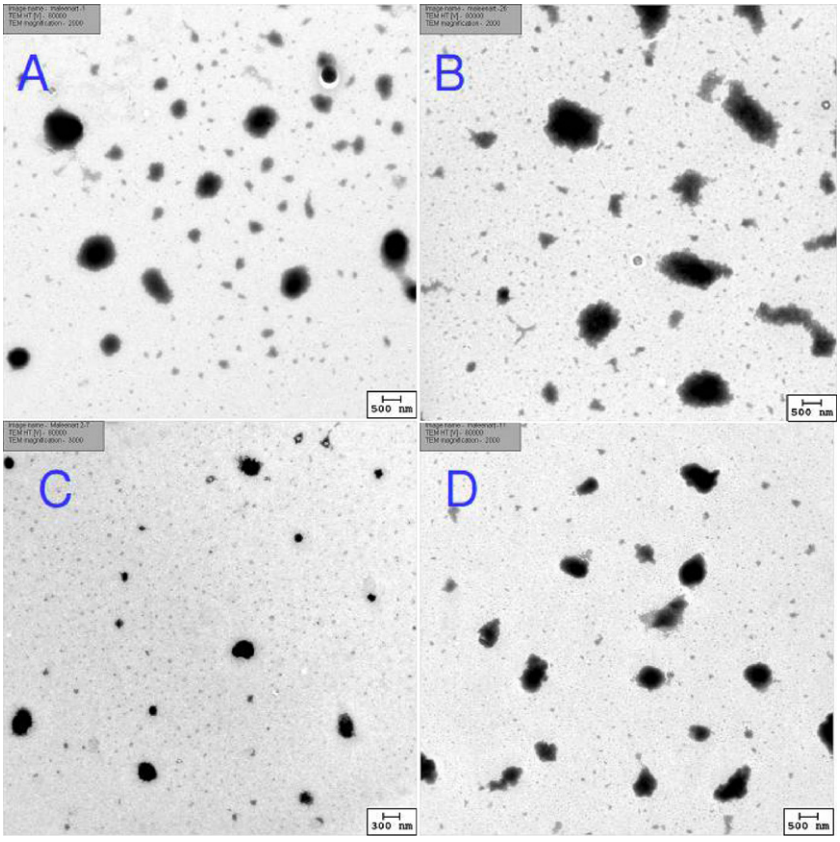

Fig. 5. TEM images of nanopolyplexes with $DQ_T = 85 \pm 2\%$ and Py/Tr = 16 ± 2: (A) M_w = 82 kDa, (B) M_w = 56 kDa and (C) 8 kDa, and with $DQ_T = 83 \pm 2\%$ and Py/Tr = 0.8 ± 2; (D) M_w = 102 kDa.

ability of nanopolyplexes to escape from endolysosomal compartment, it was correlated with the buffer capacity of the polymer in the pH range of 5–7 (Tang & Szoka, 1997). An appropriate buffer capacity of polycations is important in the design of gene vectors. The buffer capacities of M3-PyMeChC with various molecular weights and a PEI of 25 kDa were determined by an acid–base titration method (Fig. 6). The PEI showed a high buffer capacity while the M3-PyMeChC demonstrated lower buffer capacities. This could be explained by the buffer capability of the cationic polymers, which mainly depended on the presence of primary, secondary, and tertiary amine groups (Lu, Sun, Li, Zhang, & Zhuo, 2009). Therefore, the lower buffer capacity of the MPyMeChC is attributed to lower

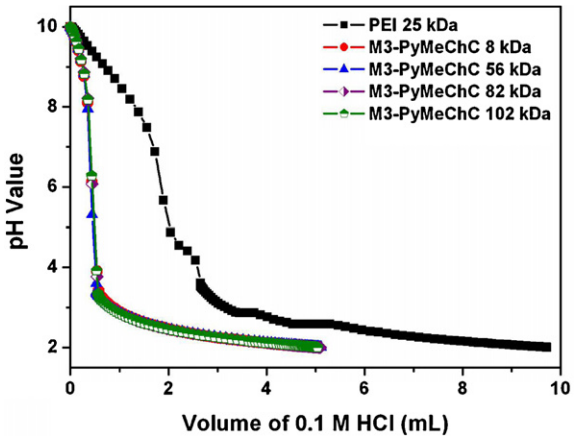

Fig. 6. Titration curve of M3-PyMeChC, with different molecular weights and Py/Tr ratios, with 0.1 M HCl. Branched PEI (M_w 25 kDa) was used as a control.

levels of the quaternary ammonium moieties on the M3-PyMeChC backbone.

3.3. *In vitro* transfection

To evaluate the potential of the synthetic polycations as gene vectors, *in vitro* transfection experiments were conducted using M3-PyMeChC/pEGFP-C2 nanopolyplexes, expressing GFP, at N/P ratios of 0.3–20 on the Huh7 cell lines. Naked DNA was used as a negative control and branched PEI (25 kDa) at an optimized N/P ratio of 8 was used as a positive control. The results are shown in Fig. 7. We found that the transfection efficiencies of nanopolyplexes in Huh7 cells were greatly depended on the N/P ratio, the molecular weight, and the type of quaternary ammonium moiety. Previously, we found that the transfection efficiency of quaternized chitosan derivatives was dependent on the DQ (Opanasopit et al., 2008). The transfection efficiency increased with an increasing DQ. However, this factor might be dependent on the type of cell lines and the cytotoxicity of the quaternized chitosan derivatives. Since cellular membrane composition varies among cellular types, it might facilitate or hinder the binding of the nanopolyplexes and subsequent internalization (Corsi, Chellat, Yahia, & Fernandes, 2003). The effect of M_w on transfection efficiencies was studied using M3-PyMeChC as a model. The M3-PyMeChC with a M_w of 82 kDa showed higher gene efficiency than that with a M_w of 56 and 8 kDa. The highest GFP expression in Huh7 cells transfected with nanopolyplexes was observed at a N/P ratios of 5. In fact, increasing the N/P ratio would increase the zeta potential of nanopolyplexes due to increasing cationic charged density. This might lead to increased cellular uptake and gene transfection; however, the nanopolyplexes with a high N/P ratio would conversely lead to decreased gene transfection due to severe cytotoxicity (Fig. 8) (Kean et al., 2005). The

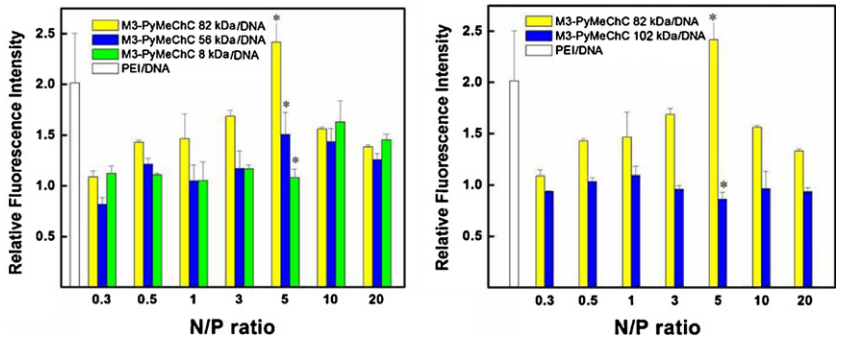

Fig. 7. *In vitro* transfection efficiencies of nanopolyplexes with different molecular weights Py/Tr ratios in Huh7 cells. Branched PEI (M_w 25 kDa) was used as a control. *$p < 0.05$ when nanopolyplexes with 82 kDa compared to nanopolyplexes with 56 kDa and 8 kDa and when nanopolyplexes with Py/Tr ratio 16 ± 2 compared to nanopolyplexes with Py/Tr ratio 0.8 ± 2. Data are represented as mean ± standard deviation ($n = 3$).

effect of the M_w of the chitosan on transfection efficiency could be described by the chain entanglement effect (Kiang et al., 2004). The high M_w of chitosan was more easily entangled with free DNA once the initial electrostatic interaction had occurred, leading to the formation of compact nanopolyplexes. Recently, Layman et al. found that higher molecular weight poly(2-dimethylaminoethyl methacrylate) showed a stronger binding affinity with plasmid DNA than lower molecular weight, leading to increased transfection efficiency. However, the question is how polycation binding affinity influences the intracellular fate of polyplexes. They suggested that the greater binding affinity helps to protect the plasmid DNA from DNase degradation, which allows greater protein expression (Layman, Ramirez, Green, & Long, 2009).

Moreover, we found that the nanopolyplexes with higher Py/Tr ratio showed higher gene efficiency than those with lower Py/Tr ratio at every N/P ratio (Fig. 7). The effect of Py/Tr ratio on transfection efficiency could be explained in terms of the hydrophobic effect. Hydrophobic moieties in the non-viral vectors are expected to increase transfection efficiency by modulating complex interactions with the cell surface (Kurisawa, Yokoyama, & Okano, 2000) and assisting dissociation of polymer/DNA nanopolyplexes, to facilitate release of DNA from vectors which otherwise would strongly bind through ionic interactions between cationic moieties and phosphates of DNA (Kim et al., 2007). In comparison to the trimethyl ammonium group, the pyridinium group has a more hydrophobic character due to the pyridine ring. In addition, the positive charge of the pyridinium group is able to spread the positive charge by delocalizing it into a heterocyclic ring, leading to enhancement of transfection efficiency. This is consistent with the results for heterocyclic cationic lipids containing imidazolium or pyridinium polar heads, which have shown higher transfection efficiencies and also reduced cytotoxicity when compared with classical transfection systems (Ilies et al., 2005, 2004; Meekel et al., 2000; Pijper et al., 2003; Roosjen et al., 2002; Solodin et al., 1995; Van Der Woude et al., 1997).

3.4. Evaluation of cytotoxicity

One of the major requirements for the cationic non-viral vectors used in gene delivery system is non-cytotoxicity. The cytotoxicity of nanopolyplexes was evaluated in Huh7 cells by MTT assay, while the PEI/DNA nanopolyplex was used as the control. The cytotoxicity of nanopolyplexes was related to the N/P ratio, the molecular weight, and the type of quaternary ammonium moiety (Fig. 8). The cytotoxicity of nanopolyplexes gradually increased with increasing of the N/P ratios due to the presence of a high amount of cationic charged density, leading to damage to the cellular membranes. When compared to high M_w, low M_w showed lower cytotoxicity, particularly at higher N/P ratios. This could be explained by each individual shorter chain of the lower M_w M3-PyMeChC having fewer contact points with the cell components (Kean et al., 2005). At similar DQ values, higher Py/Tr ratios of nanopolyplexes trended to reduce cytotoxicity compared to lower Py/Tr ratios (Fig. 8). This could be due to the chemical structure of the M3-PyMeChC and the positively charged location. Delocalization of the positive charge in the pyridinium group it might lead to a reduction in cytotoxicity. In our study, we demonstrated that at a N/P ratio of 5, the nanopolyplexes showed the highest *in vitro* transfection with 80% cell viability.

3.5. Cellular internalization

It is known that the particle charge and size affected on cellular uptake and transfection efficiency. Previously, it has been reported that nanopolyplexes can be uptaked by different pathways such as clathrin-mediated endocytosis, macropinocytosis and

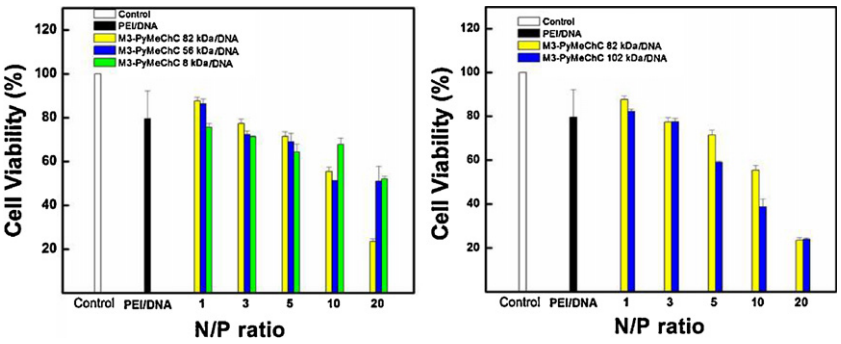

Fig. 8. *In vitro* cytotoxicity of nanopolyplexes with different molecular weights and Py/Tr ratios in Huh7 cells. Data are represented as mean ± standard deviation ($n = 3$).

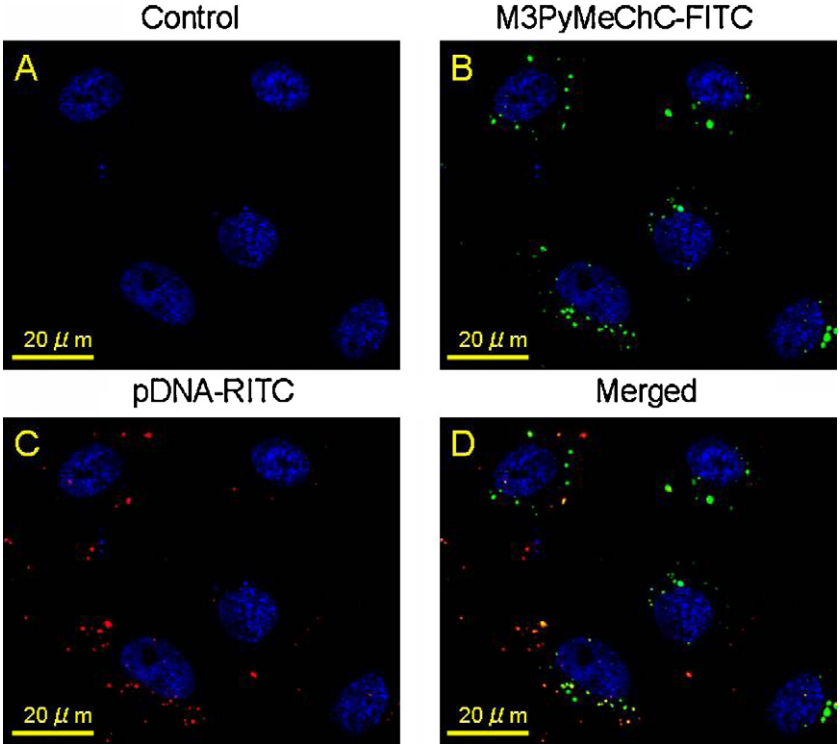

Fig. 9. Confocal laser scanning microscopy of Huh7 cells treated with nanopolyplexes with $DQ_T = 85 \pm 2\%$, Py/Tr = 16 ± 2 and M_w = 82 kDa for 24 h at 37 °C. Blue: TO-PRO-3 labeled nucleus (A), green: FITC labeled M3-PyMeChC (B), red: RITC labeled DNA (C), and merged (D). Scale bar: 20 μm. (For interpretation of the references to color in this figure legend, the reader is referred to the web version of this article.)

raft/caveolae (Goncalves et al., 2004; Manunta et al., 2006; Rejman, Bragonzi, & Conese, 2005). However, the route of nanopolyplexes uptake resulting in efficient transfection is not yet clearly identified and may depend both on the cell line and nanopolyplexes studied (Gersdorff et al., 2006; Goncalves et al., 2004; Rejman et al., 2005). Grosse et al. showed that nanopolyplexes size as well is an important determinant for uptake mechanism (Grosse et al., 2005). Most polycationics/DNA nanopolyplexes can be uptaked into a cell through the endocytosis pathway, which is limited to particles sizes of less than 150 nm in diameter (Anderson, Akinc, Hossain, & Langer, 2005; Guy, Drabek, & Antoniou, 1995). There is still disagreement over whether small or large particles will exhibit better transfection (Ogris, Steinlein, Carotta, Brunner, & Wagner, 2001). This leads to a hypothesis that apart from particle size, other biophysical parameters such as polymer structure, polymer molecular weight, and charge ratio may play an important role in transfection efficiency. However, the mechanism of cellular uptake and release of chitosan derivatives nanopolyplexes has been addressed less often. In this study, confocal laser scanning microscopy (CLSM) was used to study internalization of nanopolyplexes with a M_w of 82 kDa in Huh7 cell lines at a N/P ratio of 5. The release of DNA was detected using the fluorescent TO-PRO-3 labeled-nucleus of treated cells, RITC labeled-DNA, and FITC labeled-M3-PyMeChC, corresponding to the blue spot, the green spot, and the red spot in Fig. 9, respectively. We found that the nanopolyplexes can be intracellular around the nucleus after incubation for 24 h. The merged image indicates that the nanopolyplexes were able to be cellular uptake into cytoplasm and escaped from the endosome. The nanopolyplexes showed yellow spots which means they had a combination of the red color of the DNA and the green color of M3-PyMeChC. It is noted that if DNA has left from the M3-PyMeChC, the red spots and green spots of free DNA and M3-PyMeChC without DNA will be observed. Interestingly, our result showed that the yellow spots were less common around the nucleus. This might be due to the majority of DNA being released from nanopolyplexes. The release of nanopolyplexes from endosomes is considered to be induced by the buffering effect. The mechanism of the intracellular release of the chitosan nanopolyplex was found to be similar to that proposed for the PEI nanopolyplex (Germershaus, Mao, Sitterberg, Bakowsky, & Kissel, 2008; Hashimoto, Morimoto, Saimoto, Shigemasa, & Sato, 2006; Ishii, Okahata, & Sato, 2001). This result contrasted with our result due to the low buffering capacity of the M3-PyMeChC. However, this phenomenon is consistent with Liu and Reineke, who suggested that the buffering capacity could not effectively predict the gene delivery efficiency since the polymer structure can have a profound effect on many biological properties such as nanopolyplex stability, cellular uptake, and gene expression (Liu & Reineke, 2007). Generally, the cellular internalization of the nanopolyplexes is enhanced when the number of amines or quaternary ammonium groups is increased in the polymer repeat unit. Negatively charged proteoglycans found on the cell surface are believed to play an integral role in mediating cellular uptake of cationic polyplexes (Mislick & Baldeschwieler, 1996). However, different cell types have diverse distributions of proteoglycans on their surfaces. Even though the M3-PyMeChC had a low buffering capacity, but it had a high cationic charged density due to pyridinium moiety. This may explain why the low buffering capacity can increase the transfection efficiency. After the cellular uptake, endosomal escape could then occur through polymer proteoglycan chelation (resulting in the formation of leaky holes in the endosomal membrane, thus facilitating endosomal escape) and increased gene expression (Liu & Reineke, 2007). Hong et al. have shown that PAMAM dendrimers with terminal amine groups can strongly interact through electrostatic interactions with negatively charged phospholipids, which can induce defects in the cellular membrane and cause membrane leakage (Hong et al., 2004). Another approach suggests that the endosomal escape of high M_w chitosan nanopolyplexes depends on enzymatic-degradation of chitosan rather than a proton buffering

capacity that would occur less readily with high DD. The resulting degradation fragments (oligo- and monosaccharides) are hypothesized to increase endosome osmolarity and lead to membrane rupture. In addition, Verheul et al. demonstrated that the rate of enzymatic degradation of trimethyl chitosan chloride (TMC) by lysozyme decreases proportionally to the DQ (Verheul et al., 2009). However, our result confirmed that the DNA could escape from M3-PyMeChC and move to the nucleus.

4. Conclusion

We demonstrated the effects of molecular weight and pyridinium/trimethyl (Py/Tr) ratios on transfection efficiency and cytotoxicity. In this study, the M3-PyMeChC with a higher molecular weight and Py/Tr ratio showed enhancement of transfection efficiency at a N/P ratio of 5. However, higher molecular weight tended to increase cytotoxicity while higher Py/Tr ratios reduced cytotoxicity, although this was also depended on the N/P ratio. The improvement of transfection efficiency might be due to hydrophobic effects, leading to easy dissociation of DNA from nanopolyplexes which confirmed using confocal laser scanning microscopy. Since the pyridinium moiety can spread the positive charge by delocalizing it into a heterocyclic ring, it results in a reduction in cytotoxicity. We also demonstrated that a low buffering capacity can increase the transfection efficiency. This might take place via a polymer proteoglycan chelation mechanism, leading to leaky holes in the endosomal membrane. Our results showed that the chemical structure of the pyridinium moiety, the molecular weight, and the N/P ratio, play an important role in transfection efficiency and cytotoxicity.

Acknowledgments

We gratefully acknowledge financial support from the Research, Development and Engineering (RD&E) Fund through the National Nanotechnology Center (NANOTEC), National Science and Technology Development Agency (NSTDA), Thailand (Project No. NN-B-22-EN4-94-51-10).

References

Anderson, W. F. (1992). Human gene therapy. *Science*, *256*, 808–813.
Anderson, D. G., Akinc, A., Hossain, N., & Langer, R. (2005). Structure/property studies of polymeric gene delivery using a library of poly(β-amino esters). *Molecular Therapy*, *11*, 426–434.
Benns, J. M., Choi, J. S., Mahato, R. I., Park, J. S., & Kim, S. W. (2000). pH-sensitive cationic polymer gene delivery vehicle: *N*-Ac-poly(L-histidine)-graft-poly(L-lysine) comb shaped polymer. *Bioconjugate Chemistry*, *11*, 637–645.
Boussif, O., Lezoualc'h, F., Zanta, M. A., Mergny, M. D., Scherman, D., Demeneix, B., et al. (1995). A versatile vector for gene and oligonucleotide transfer into cells in culture and in vivo: Polyethylenimine. *The Proceedings of the National Academy of Sciences of the United States of America*, *92*, 7297–7301.
Corsi, K., Chellat, F., Yahia, L., & Fernandes, J. C. (2003). Mesenchymal stem cells, MG63 and HEK293 transfection using chitosan–DNA nanoparticles. *Biomaterials*, *24*, 1255–1264.
Farber, I. Y., & Domb, A. J. (2007). Cationic polysaccharides for gene delivery. *Materials Science and Engineering C*, *27*, 595–598.
Gao, X., Kim, K. S., & Liu, D. (2007). Nonviral gene delivery: What we know and what is next. *The American Association Pharmaceutical Scientists Journal*, *9*, E92–E104.
Germershaus, O., Mao, S., Sitterberg, J., Bakowsky, U., & Kissel, T. (2008). Gene delivery using chitosan, trimethyl chitosan or polyethylenglycol-graft-trimethyl chitosan block copolymers: Establishment of structure–activity relationships in vitro. *Journal of Controlled Release*, *125*, 145–154.
Gersdorff, K. V., Sanders, N. N., Vandenbroucke, R., De Smedt, S. C., Wagner, E., & Ogris, M. (2006). The internalization route resulting in successful gene expression depends on both cell line and polyethylenimine polyplex type. *Molecular Therapy*, *14*, 745–753.
Goncalves, C., Mennesson, E., Fuchs, R., Gorvel, J. P., Midoux, P., & Pichon, C. (2004). Macropinocytosis of polyplexes and recycling of plasmid via the clathrin-dependent pathway impair the transfection efficiency of human hepato-carcinoma cells. *Molecular Therapy*, *10*, 373–385.
Green, J. J., Langer, R., & Anderson, D. G. (2008). A combinatorial polymer library approach yields insight into non-viral gene delivery. *Accounts of Chemical Research*, *41*, 749–979.
Grosse, S., Aron, Y., Thevenot, G., Francois, D., Monsigny, M., & Fajac, I. (2005). Potocytosis and cellular exit of complexes as cellular pathways for gene delivery by polycations. *The Journal of Gene Medicine*, *7*, 1275–1286.
Guy, J., Drabek, D., & Antoniou, M. (1995). Delivery of DNA into mammalian cells by receptor-mediated endocytosis and gene therapy. *Molecular Biotechnology*, *3*, 237–248.
Hashimoto, M., Morimoto, M., Saimoto, H., Shigemasa, Y., & Sato, T. (2006). Lactosylated chitosan for DNA delivery into hepatocytes: The effect of lactosylation on the physicochemical properties and intracellular trafficking of pDNA/chitosan complexes. *Bioconjugate Chemistry*, *17*, 309–316.
Hong, S., Bielinska, A. U., Mecke, A., Keszler, B., Beals, J. L., Shi, X., et al. (2004). Interaction of poly(amidoamine) dendrimers with supported lipid bilayers and cells: Hole formation and the relation to transport. *Bioconjugate Chemistry*, *15*, 774–782.
Huang, M., Khor, E., & Lim, L. Y. (2004). Uptake and cytotoxicity of chitosan molecules and nanoparticles: Effects of molecular weight and degree of deacetylation. *Pharmaceutical Research*, *21*, 344–353.
Jayakumar, R., Chennazhi, K. P., Muzzarelli, R. A. A., Tamura, H., Nair, S. V., & Selvamurugan, N. (2010). Chitosan conjugated DNA nanoparticles in gene therapy. *Carbohydrate Polymers*, *79*, 1–8.
Ilies, M. A., Johnson, B. H., Makori, F., Miller, A., Seitz, W. A., Thompson, E. B., et al. (2005). Pyridinium cationic lipids in gene delivery: An in vitro and in vivo comparison of transfection efficiency versus a tetraalkylammonium congener. *Archives of Biochemistry Biophysics*, *435*, 217–226.
Ilies, M. A., Seitz, W. A., Ghiviriga, I., Johnson, B. H., Miller, A., Thompson, E. B., et al. (2004). Pyridinium cationic lipids in gene delivery: A structure–activity correlation study. *Journal of Medicinal Chemistry*, *47*, 3744–3754.
Ishii, T., Okahata, Y., & Sato, T. (2001). Mechanism of cell transfection with plasmid/chitosan complexes. *Biochimica et Biophysica Acta*, *1514*, 51–64.
Janes, K. A., & Alonso, M. J. (2003). Depolymerized chitosan nanoparticles for protein delivery: Preparation and characterization. *Journal of Applied Polymer Science*, *88*, 2769–2776.
Kean, T., Roth, S., & Thanou, M. (2005). Trimethylated chitosans as non-viral gene delivery vectors: Cytotoxicity and transfection efficiency. *Journal of Controlled Release*, *103*, 643–653.
Kiang, T., Wen, J., Lim, H. W., & Leong, K. W. (2004). The effect of the degree of chitosan deacetylation on the efficiency of gene transfection. *Biomaterials*, *25*, 5293–5301.
Kim, T. H., Jiang, H. L., Jere, D., Park, I. K., Cho, M. H., Nah, J. W., et al. (2007). Chemical modification of chitosan as a gene carrier in vitro and in vivo. *Progress in Polymer Science*, *32*, 726–753.
Knight, D. K., Shapka, S. N., & Amsden, B. G. (2007). Structure, depolymerization, and cytocompatibility evaluation of glycol chitosan. *Journal of Biomedical Materials Research Part A*, *83*, 787–798.
Kurisawa, M., Yokoyama, M., & Okano, T. (2000). Transfection efficiency increases by incorporating hydrophobic monomer units into polymeric gene carriers. *Journal of Controlled Release*, *68*, 1–8.
Layman, J. M., Ramirez, S. M., Green, M. D., & Long, T. E. (2009). Influence of polycation molecular weight on poly(2-dimethylaminoethyl methacrylate)-mediated DNA delivery in vitro. *Biomacromolecules*, *10*, 1244–1252.
Li, S., & Huang, L. (2000). Nonviral gene therapy: Promises and challenges. *Gene Therapy*, *7*, 31–34.
Liu, Y., & Reineke, T. M. (2007). Poly(glycoamidoamine)s for gene delivery. Structural effects on cellular internalization, buffering capacity, and gene expression. *Bioconjugate Chemistry*, *18*, 19–30.
Lu, B., Sun, Y. X., Li, Y. Q., Zhang, X. Z., & Zhuo, R. Z. (2009). *N*-succinyl-chitosan grafted with low molecular weight polyethylenimine as a serum-resistant gene vector. *Molecular Biosystems*, *5*, 629–637.
Manunta, M., Nichols, B. J., Hong Tan, P., Sagoo, P., Harper, J., & George, A. J. (2006). Gene delivery by dendrimers operates via different pathways in different cells, but is enhanced by the presence of caveolin. *Journal of Immunological Methods*, *314*, 134–146.
Meekel, A. A. P., Wagenaar, A., Smisterova, J., Kroeze, J. E., Haadsma, P., Bosgraaf, B., et al. (2000). Synthesis of pyridinium amphiphiles used for transfection and some characteristics of amphiphile/DNA complex formation. *European Journal of Organic Chemistry*, *4*, 665–673.
Mislick, K. A., & Baldeschwieler, J. D. (1996). Evidence for the role of proteoglycans in cation-mediated gene transfer. *The Proceedings of the National Academy of Sciences of the United States of America*, *93*, 12349–12354.
Ogris, M., Steinlein, P., Carotta, S., Brunner, S., & Wagner, E. (2001). DNA/polyethylenimine transfection particles: Influence of ligands, polymer size and PEGylation on internalisation and gene expression. *The American Association Pharmaceutical Scientists PharmSci*, *3*, 43–53.
Opanasopit, P., Sajomsang, W., Ruktanonchai, U., Mayen, V., Rojanarata, T., & Ngawhirunpat, T. (2008). Methylated *N*-(4-pyridinylmethyl) chitosan as a novel effective safe gene carrier. *International Journal of Pharmaceutics*, *364*, 127–134.
Pijper, D., Bulten, E., Šmisterová, J., Wagenaar, A., Hoekstra, D., Engberts, J. B. F. N., et al. (2003). Novel biodegradable pyridinium amphiphiles for gene delivery. *European Journal of Organic Chemistry*, *22*, 4406–4412.
Rejman, J., Bragonzi, A., & Conese, M. (2005). Role of clathrin- and caveolae-mediated endocytosis in gene transfer mediated by lipo- and polyplexes. *Molecular Therapy*, *12*, 468–474.

Roosjen, A., Šmisterová, J., Driessen, C., Anders, J. T., Wagenaar, A., Hoekstra, D., et al. (2002). Synthesis and characteristics of biodegradable pyridinium amphiphiles used for in vitro DNA delivery. *European Journal of Organic Chemistry*, *7*, 1271–1277.

Sajomsang, W., Ruktanonchai, U., Gonil, P., Mayen, V., & Opanasopit, P. (2009). Methylated *N*-aryl chitosan derivative/DNA complex nanoparticles for gene delivery: Synthesis and structure–activity relationships. *Carbohydrate Polymers*, *78*, 743–752.

Sajomsang, W., Rungsardthong Ruktanonchai, U., Gonil, P., & Warin, C. (2010). Quaternization of *N*-(3-pyridylmethyl) chitosan derivatives: Effects of the degree of quaternization, molecular weight and ratio of *N*-methylpyridinium and *NNN*-trimethyl ammonium moieties on bactericidal activity. *Carbohydrate Polymers*, *82*, 1143–1152.

Solodin, I., Brown, C. S., Bruno, M. S., Chow, C. Y., Jang, E. H., Debs, R. J., et al. (1995). A novel series of amphiphilic imidazolinium compounds for in vitro and in vivo gene delivery. *Biochemistry*, *34*, 13537–13544.

Tang, M. X., & Szoka, F. C. (1997). The influence of polymer structure on the interactions of cationic polymers with DNA and morphology of the resulting complexes. *Gene Therapy*, *4*, 823–832.

Van Der Woude, I., Wagenaar, A., Meekel, A. A. P., Ter Beest, M. B. A., Ruiters, M. H. J., Engberts, J. B. F. N., et al. (1997). Novel pyridinium surfactants for efficient, nontoxic in vitro gene delivery. *The Proceedings of the National Academy of Sciences of the United States of America*, *94*, 1160–1165.

Verheul, R. J., Amidi, M., van Steenbergen, M. J., van Riet, E., Jiskoot, W., & Hennink, W. E. (2009). Influence of the degree of acetylation on the enzymatic degradation and in vitro biological properties of trimethylated chitosans. *Biomaterials*, *30*, 3129–3135.

Weecharangsan, W., Opanasopit, P., Ngawhirunpat, T., Rojanarata, T., & Apirakaramwong, A. (2006). Chitosan lactate as a nonviral gene delivery vector in COS-1 cells. *The American Association Pharmaceutical Scientists PharmSciTech*, *7*, E74–E79.